Surface Roughness of Topography: A Multi-Scale Analysis of Landform Elements in Midland Valley, Scotland

C. H. Grohmann[1], M. J. Smith[2], C. Riccomini[3]

[1] Institute of Geosciences – University of São Paulo – Rua do Lago, 562, São Paulo, SP, Brazil, 05508-080
Telephone: +55 11 3091- 4216
Fax: +55 11 3091-4258
Email: guano@usp.br, carlos.grohmann@gmail.com

[2] School of Geography, Geology and the Environment, Kingston University, Kingston-upon-Thames, Surrey, KT1 2EE, UK
Telephone: +44 (0) 207 099 2817
Fax: +44 (0) 870 063 3061
Email:michael.smith@kingston.ac.uk

[3] Institute of Geosciences – University of São Paulo – Rua do Lago, 562, São Paulo, SP, Brazil, 05508-080
Telephone: +55 11 3091- 4126
Fax: +55 11 3091-4207
Email: riccomin@usp.br

1. Introduction

Surface roughness is a key variable used across the earth and planetary sciences (Hobson 1972) to both identify individual landforms and determine the processes acting upon them. In geomorphometry, roughness is described using surface elevation values and can be used to characterise landforms over a variety of different scales.

Throughout this article, we use the term *surface roughness* as an expression of the variability of elevation of a topographic surface *at a given scale*, where the scale of analysis is determined by the size of the landforms or geomorphic features of interest, either local or regional.

In this paper we briefly review a selection of measures of surface roughness, with specific application to grid based digital elevation models (DEMs). A selection were assessed for the behaviour of roughness at different spatial scales and dataset resolutions using moving-window and raster algebra steps to a test area in the Midland Valley, Scotland.

1.1 Measures of Surface Roughness

The *area ratio* evaluates the similarities between the surface (real) area and flat (plan) area of square cells or triangles defined by input points, by calculating the ratio of these values. According to Hobson (1972) flat surfaces would present values close to one, whilst with irregular surfaces the ratio shows a curvilinear relationship which asymptotically approaches infinity as the real area increases.

Different measurements of *vector dispersion* (or orientation) were used as a proxy for surface roughness (e.g., Hobson 1972; Day 1979; Guth 2003; McKean and Roering 2004). An array of regularly spaced elevation values can be divided into planar triangular surfaces and normals to these planes represented by unit vectors. Values of vector mean, strength (R) and dispersion (k) can be calculated for each square cell. In smooth areas, with similar elevations, vector strength is expected to be high and vector dispersion to be low, since the vectors will become parallel, as R approaches N. In rough areas, the non-systematic variation in elevation readings will result in low vector strength and high vector dispersion.

Several authors define surface roughness in terms of the *variability of elevation* values, generally expressed as the absolute standard deviation of all values within a window, or as the deviation from a best-fit plane (e.g, Haneberg et al., 2005, Frankel and Dolan 2007, Evans 1984). As the *slope* denotes the rate of change of elevation, *profile curvature (profc)* measures the rate of change of slope. Area ratio, vector dispersion, SD_{elev}, SD_{slope} and SD_{profc} were selected for further study.

The selected methods are suited to array-based calculations using DEMs as primary input data and were implemented as shell scripts in GRASS-GIS (Neteler and Mitasova 2007, GRASS Development Team 2008) as sequences of neighbourhood (i.e. moving-window) and raster map algebra analysis steps.

Moving-window operators were adopted because the morphometric parameter is calculated for all input cells, so there is no risk of ”missing" any terrain feature (Grohmann and Riccomini 2009). The flexibility of array-based calculations also means that a multi-scale study can be performed simply by changing the neighbourhood size.

2. Methodology and Study Area

A study area located in the Midland Valley, Scotland (Fig. 1), was selected. The NEXTMap Britain (Smith et al., 2006) DEM was considered suitable as the input dataset. This product was acquired and produced by Intermap Technologies using airborne InSAR at a spatial resolution of 5 m.

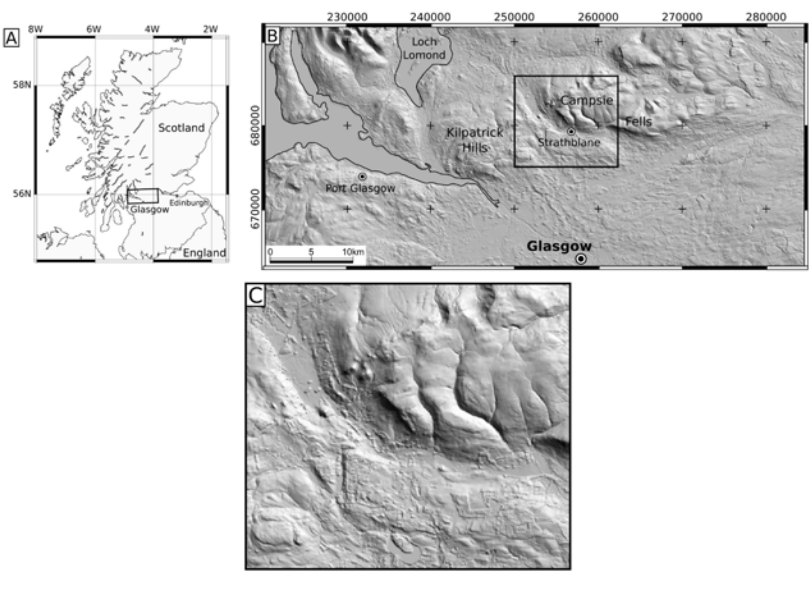

Figure 1. Shaded relief image depicting the location of the study area (illumination 045º, elevation 30º, no vertical exaggeration).

To evaluate the effects of spatial resolution, the original DEM was resampled by calculating the mean elevation value at resolutions of 10, 25, 50 and 100 m. To evaluate scale effects of roughness, the selected methods were applied to all DEMs using moving-windows of 3x3, 5x5, 7x7, 9x9, 11x11, 13x13, 15x15, 17x17, 19x19, 21x21, 31x31 and 51x51 cells. Roughness was calculated for the 5 resolutions and 12 window sizes, giving a total of 300 individual model runs.

To calculate area ratio, the surface area of individual cells was calculated from the trigonometric relationships between the square (horizontal) pixel and its inclined projection, given by slope (Grohmann 2004).

To calculate vector strength (R) and dispersion ($1/k$), compass-oriented aspect, colatitude (90^o-*slope*), direction cosines (Equation 1) and sum of direction cosines in a neighbourhood (Equation 2) were calculated. Vector strength was derived according to equation 3 and vector dispersion as the inverse of equation 4.

$$x_i = \sin\theta_i \cos\varphi_i \qquad y_i = \sin\theta_i \sin\varphi_i \qquad z_i = \cos\theta_i \tag{1}$$

$$\bar{x} = \sum_{i=1}^{N} x_i \qquad \bar{y} = \sum_{i=1}^{N} y_i \qquad \bar{z} = \sum_{i=1}^{N} z_i \tag{2}$$

$$R = \sqrt{\bar{x}^2 + \bar{y}^2 + \bar{z}^2} \tag{3}$$

$$k = (N - 1)/(N - R) \tag{4}$$

Standard deviation outputs were calculated using common moving-window tools.

3. Results and Discussion

Initial results are depicted in Fig. 2 A-D, where surface roughness, calculated using a 11x11 moving-window over the DEM with 10 m spatial resolution, are presented for the selected methods (area ratio, vector dispersion, SD_{elev}, SD_{slope} and SD_{profc}). Shades of yellow correspond to smoother areas, green-blue tones to intermediate values and purple-red to rough areas. It should be noted that the original roughness values were normalized, in order to provide a direct comparison of the maps.

For the area ratio output (Fig. 2A), the predominance of cyan-blue tones indicates that this method fails to distinguish features with similar elevation. The scarps of Campsie Fells are marked with high roughness values, since they have steep slope angles, even though they may be considered as smooth [inclined] surfaces.

For the vector dispersion output (Fig. 2B), the predominance of blue-purple tones indicates the sensitivity of this method to short-scale (i.e. local) variations in elevation, which are common in InSAR datasets over vegetated and urban areas. In this image the scarps of the Campsie Fells are depicted as smooth areas, with low vector dispersion.

The output for SD_{elev} (Fig. 2C) shows a predominance of low values (yellow-green tones), with the scarps of the Campsie Fells marked with high values due to the steep slopes. This method is also sensitive to local strong variations in elevation, which can be caused by spurious data.

SD_{slope} (Fig. 2D) is sensitive to sudden changes in the original slope values, and highlights the boundaries of urban and forest areas. The scarps of the Campsie Fells are correctly identified as smooth areas, with high values located over the slope break, indicating that this method is suitable for terrain analysis.

SD_{profc} (FigFig. 2E) does not identify the slope break of the Campsie Fells scarps. The higher values are found in urban and vegetated areas, indicating a sensitivity to strong variations in slope, as seen in urban features.

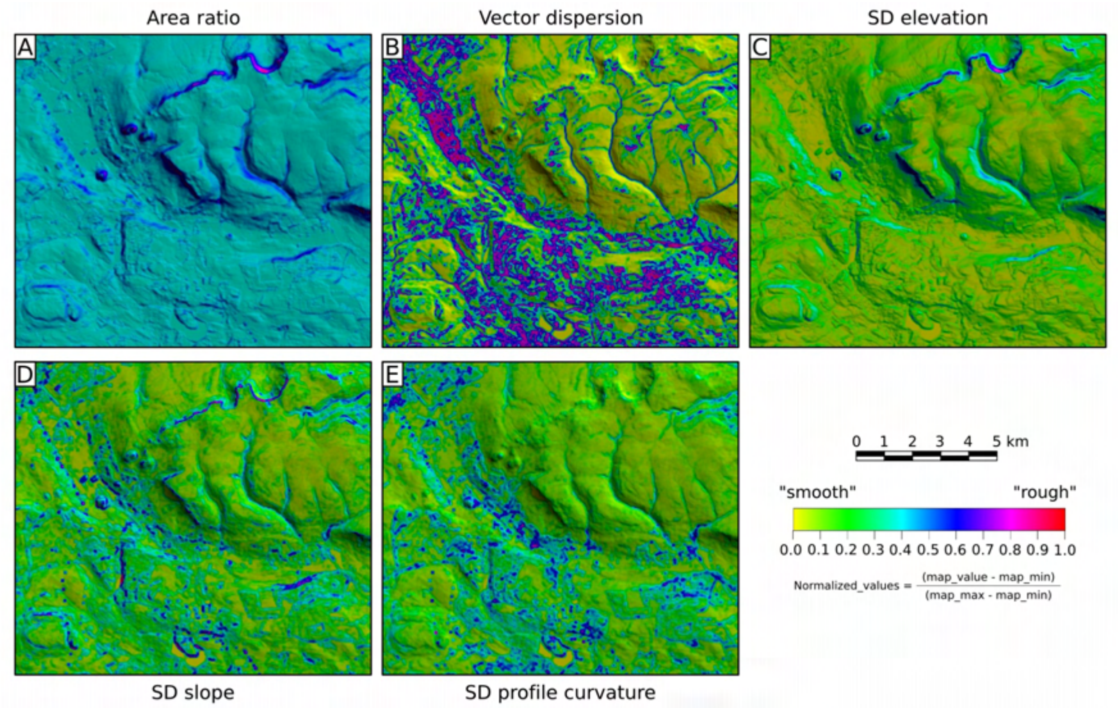

Figure 2. Sample output for surface roughness calculations. A) area ratio; B) vector dispersion (*1/k*); C) standard deviation of elevation ; D) standard deviation of slope; E) standard deviation of profile curvature. All outputs were calculated using a 11x11 neighbourhood for the 10 m DEM.

Fig. 3 shows the effect of changing the spatial resolution of the DEM for vector dispersion and SD_{slope}. Fig. 4 shows the effect of changing the moving-window size for vector dispersion and SD_{slope}. Fig. 5 depicts density plots of window size at four DEM resolutions (10, 25, 50 and 100 m) for all selected methods.

Our tests demonstrate that for area ratio the broad pattern of roughness does not change across scales or window sizes. Whilst smoothing does occur at coarser resolutions and larger window sizes, area ratio is generally scale independent.

The results for vector dispersion show a more complex relationship with resolution and window size. As resolution decreases and window size increases, roughness increases. Whilst vector dispersion is less sensitive to outliers, it only depicts roughness at certain scales and doesn't identify regional roughness features (i.e. mountain blocks). Unlike area ratio, it does (correctly) depict uniform slopes as smooth.

SD_{elev} shows an increase in roughness as resolution and window size increases, with the effect greater at coarser resolutions. In particular, breaks-of-slope are identified so that at coarser resolutions and larger window sizes, regional relief is identified.

SD_{slope} shows an increase in roughness as resolution and window size increases. Density plots exhibit a transition from unimodal distributions to bimodal or multimodal distributions with increasing window size, a behaviour enhanced at low spatial resolutions.

SD_{profc} shows a fast increase in roughness as window size increases even with moderately high resolution (20 m), Interestingly, with 50 m spatial resolution, density curves for windows from 11x11 to 21x21 pixels present a peak at about the same value.

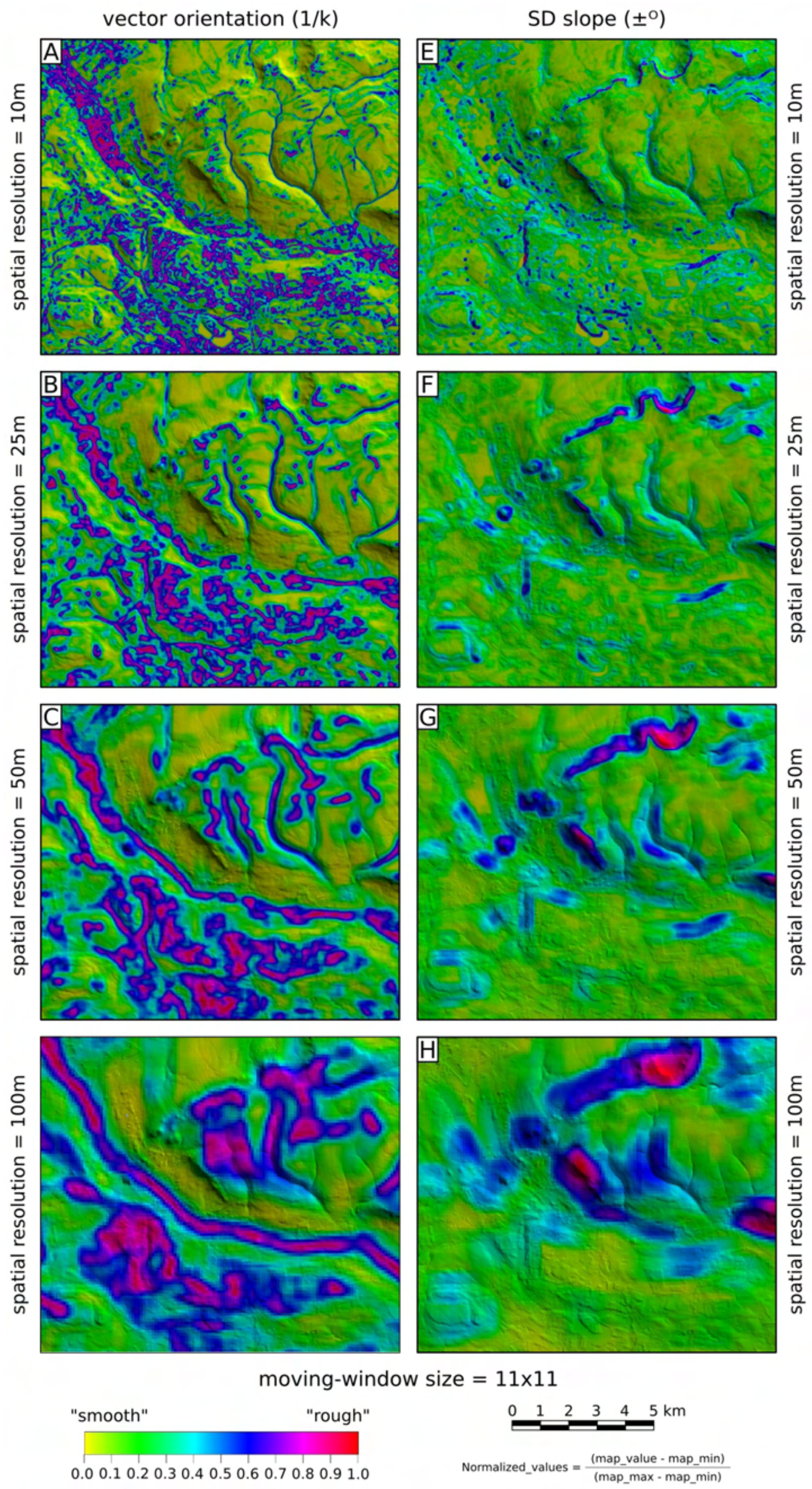

Figure 3. Effect of changing spatial resolution of the input DEM. Vector dispersion and SD_{slope} calculated using a 11x11 moving window.

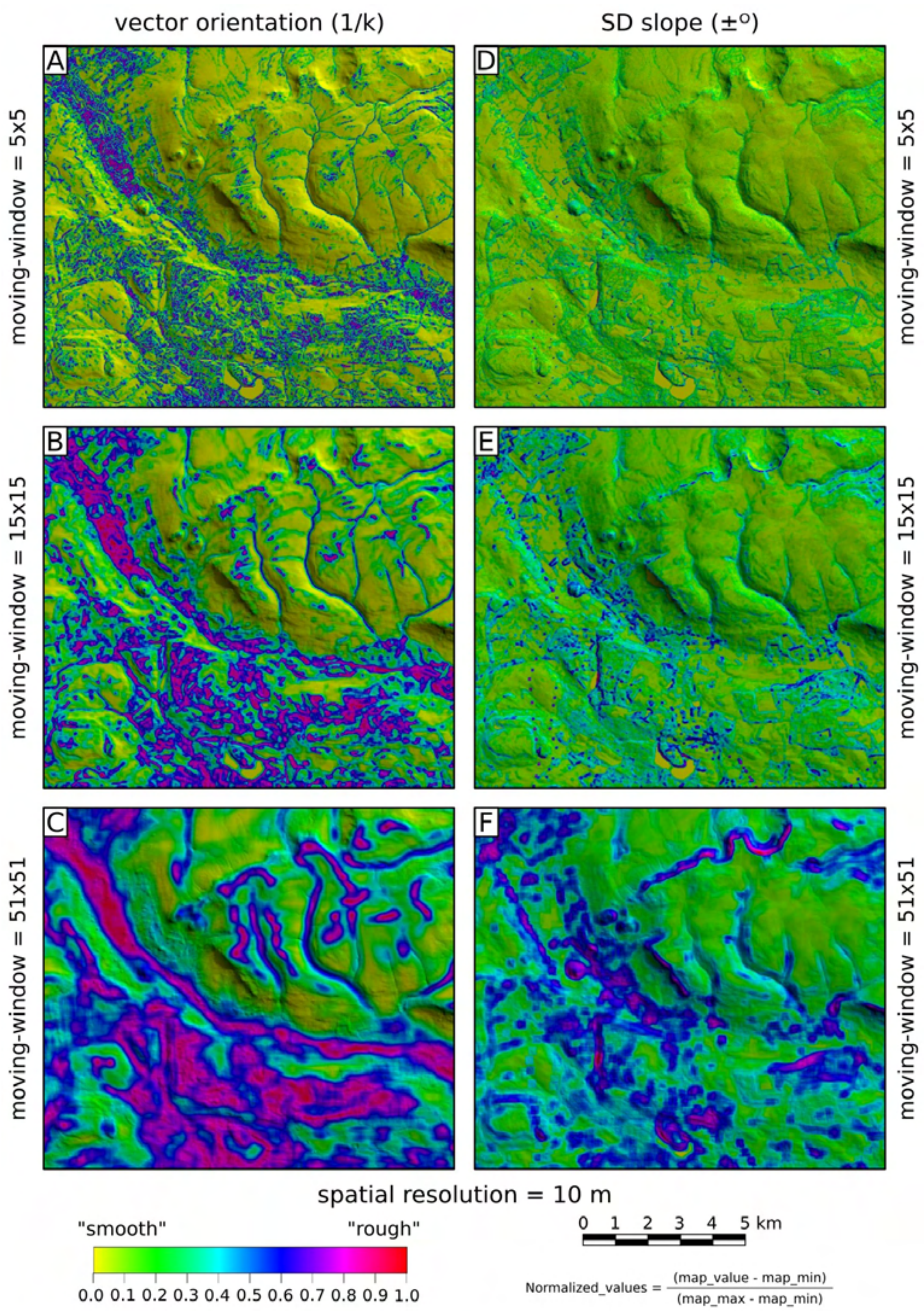

Figure 4. Effect of changing moving-window size for vector dispersion (A-C) and SD_{slope} (D-F). Output is calculated over the DEM with 10 m spatial resolution.

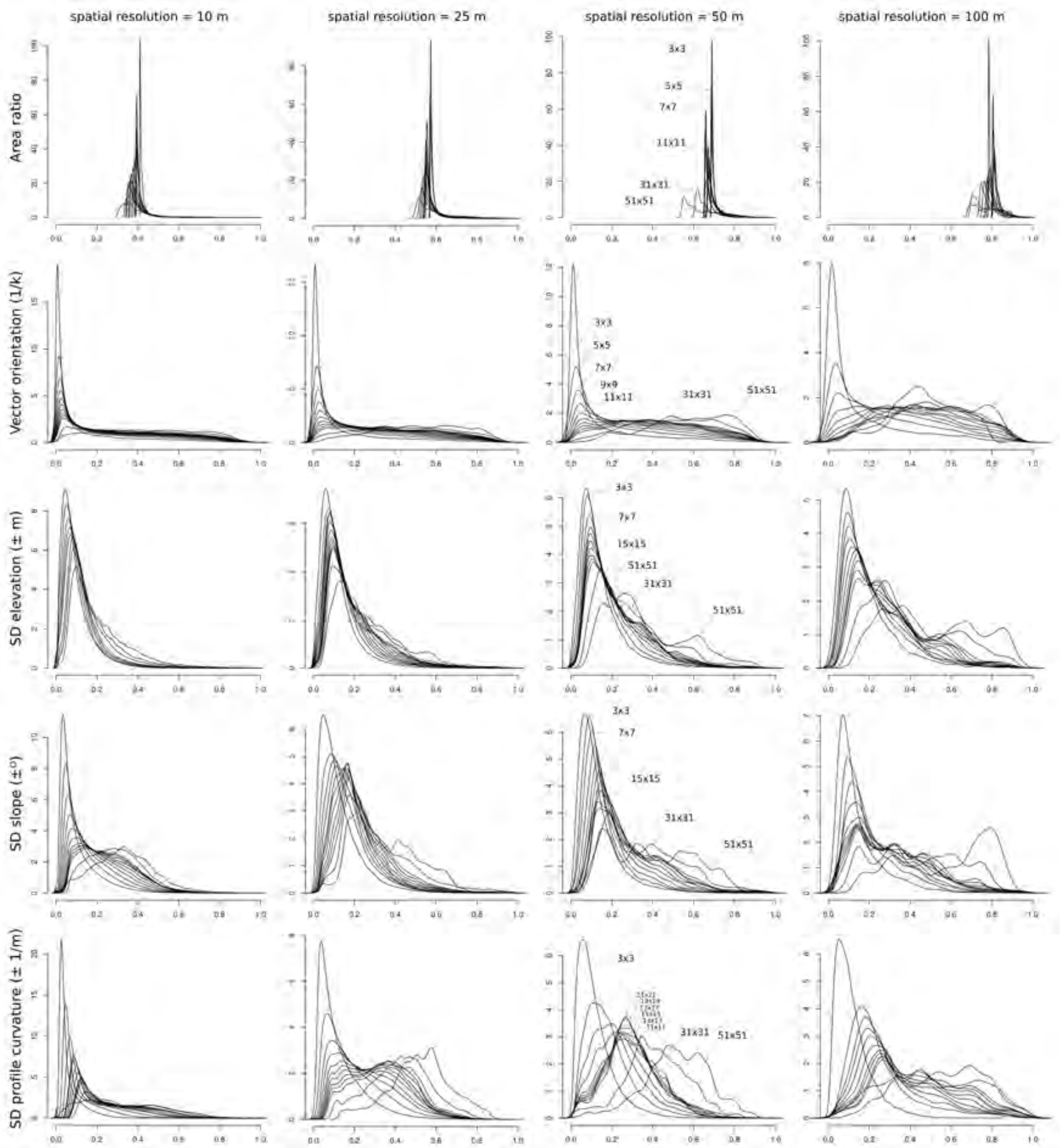

Figure 5. Density curves for the selected roughness methods plotted at four spatial resolutions (10, 25, 50 and 100 m) for 12 moving window sizes.

4. Conclusions

There is a general trend of inclusion (or exclusion) of features into homogenous neighbourhoods at coarser resolutions and larger window sizes. Large landscape elements are not depicted by small neighbourhoods while local, "fine scale", features are obliterated over wide areas. Spatial resolution is important here when, for example, studying landforms hundreds of metres wide. In this instance there is little advantage in using a detailed, fine-resolution DEM, as a large neighbourhood will be required and the number of cells within the window grows exponentially. This dramatically increases the computational time involved in roughness calculations.

In summary, area ratio operates independently of scale, providing a consistent result which means that coarser resolution DEMs should produce similar results to detailed DEMs. This is a significant advantage, although it should be noted that steep, smooth, slopes will appear as rough terrain and that this method fails in distinguishing features with similar elevations.

Vector dispersion produces a much wider range of results with increasing roughness (and homogenization of terrain) at coarser resolutions and larger window sizes. Whilst steep, smooth, slopes will have low roughness values, breaks-of-slope are not readily delimited and regional relief is more difficult to identify. However vector dispersion is good at identifying fine-scale roughness features and there is the potential for its use in automating the removal of "surface clutter" from DEMs.

SD_{elev} identifies breaks-of-slope and is therefore good at detecting regional relief. Even at fine resolutions and small window sizes it remains good at identifying small features, although standard image processing techniques (such as contrast stretches) may be required to emphasise them.

Finally, SD_{slope} correctly identifies steep smooth slopes and areas of "surface clutter" (e.g. forest stands) whilst also identifying breaks-of-slope across scales.

SD_{profc} does not identify breaks-of-slope, and is very sensitive to sudden changes in slope, as seen in urban features.

In addition to good performance at a variety of scales, both SD_{elev} and SD_{slope} benefit from the simplicity of the calculation which is perhaps their single greatest benefit. A final word of caution should be exercised with the use of output from SD_{slope} as any noise or error in the original elevation data may be enhanced.

Acknowledgements

This study was supported by CAPES/PDEE-BEX Grant 5176/06-9 and FAPESP Grant 04/06260-5 to Grohmann. Riccomini is a Research Fellow of CNPq, Grant 304649/2005-8. We gratefully acknowledge Intermap Technologies for the supply of NextMap Britain data.

References

Day MJ, 1979, Surface roughness as a discriminator of tropical karst styles. *Zeitschrift fur Geomorphologie*, Suppl.-Bd. 32:1–8.

Evans IS, 1984, Correlation structures and factor analysis in the investigation of data dimensionality: statistical properties of the Wessex land surface, England. *International Symposium on Spatial Data Handling*, Zurich, 1:98–116.

Frankel KL and Dolan JF, 2007, Characterizing arid region alluvial fan surface roughness with airborne laser swath mapping digital topographic data. *Journal of Geophysical Research (Earth Surface)*, 112:F02025.

GRASS Development Team 2008, *Geographic Resources Analysis Support System (GRASS GIS)* Software, version 6.3.0. http://www.grass.osgeo.org

Grohmann CH, 2004, Morphometric analysis in Geographic Information Systems: applications of free software GRASS and R., *Computers & Geosciences*, 30:1055–1067.

Grohmann CH and Riccomini C, 2009, Comparison of roving-window and search-window techniques for characterising landscape morphometry. *Computers & Geosciences, in press*. DOI: 10.1016/j.cageo.2008.12.014

Guth PL, 2003, Concepts and Modelling in Geomorphology: International Perspectives, chapter *Eigenvector Analysis of Digital Elevation Models in a GIS: Geomorphometry and Quality Control,* page 199-220. TERRAPUB, Tokyo.

Haneberg WC, Creighton AL, Medley EW and Jonas DA, 2005, Use of LiDAR to assess slope hazards at the Lihir gold mine, Papua New Guinea. In: Hungr O, Fell R, Couture R, and Eberhardt E, (eds), *Proceedings of International Conference on Landslide Risk Management,* Vancouver, Canada, Supplementary CD.

Hobson RD, 1972, Surface roughness in topography: quantitative approach. In Chorley, R. J., editor, *Spatial analysis in geomorphology*, pages 225–245. Methuer, London.

McKean J and Roering J, 2004, Objective landslide detection and surface morphology mapping using high-resolution airborne laser altimetry. *Geomorphology*, 57:331 351.

Neteler M and Mitasova H, 2007, *Open Source GIS : A GRASS GIS Approach*, Third Edition (The Kluwer International Series in Engineering and Computer Science), volume 773. Springer.

Smith MJ, Rose J, and Booth S, 2006, Geomorphological mapping of glacial landforms from remotely sensed data: An evaluation of the principal data sources and an assessment of their quality. *Geomorphology*, 76:148–165.